International Journal of Undergraduate Research and Creative Activities

Volume 8 Article 3

April 2016

Computational Modelling of a Spanning Drop in a Wedge with Variable Angle

Caio Rondon
Federal University of ABC, caionaudhiz@gmail.com

Valerio Ramos Batista
Federal University of ABC, vramos1970@gmail.com

Recommended Citation
Rondon, Caio and Ramos Batista, Valerio (2016) "Computational Modelling of a Spanning Drop in a Wedge with Variable Angle," *International Journal of Undergraduate Research and Creative Activities*: Vol. 8, Article 3.
DOI: http://dx.doi.org/10.7710/2168-0620.1064

Computational Modelling of a Spanning Drop in a Wedge with Variable Angle

Peer Review
This work has undergone a double-blind review by a minimum of two faculty members from institutions of higher learning from around the world. The faculty reviewers have expertise in disciplines closely related to those represented by this work. If possible, the work was also reviewed by undergraduates in collaboration with the faculty reviewers.

Abstract
In this work, mathematical and computational techniques were used to model the phenomenon of a bubble or liquid drop as it slides to the narrowest side between two tilted plates. Practical applications of this phenomenon, such as the adjustment of liquid propellant tanks, are also discussed. Computations involved the use of *Surface Evolver*—a fully open, interactive program that allows the simulation of physical experiments in a virtual environment.

Keywords
Surface Evolver, Computational Modeling, Spanning Drop, Wedge

Acknowledgements
Editor's Note: Dr. Valério Ramos Batista, Associate Professor, Federal University of ABC, served as faculty mentor for this work.

INTRODUCTION

It is frequently easy to perform experiments with bubbles and soap films, which show intriguing behaviors. For instance, two co-axial parallel rings spanned by a soap film can produce a surface called a *catenoid*. This is a surface of revolution around the axis of the rings, and its name derives from *catenary*, which is the natural curve that a chain forms when its extremes are fixed at a certain height. The word *chain* is *catena* in Italian, and this explains the origin of the name. Besides the catenoid, two parallel rings can also be spanned by another continuous soap film, as illustrated by Isenberg (1978). However, this example is not entirely smooth due to its triple junctions.

A catenoid is also formed when two parallel plates are bridged by a soap film (Figure 1). A very curious fact is that, if

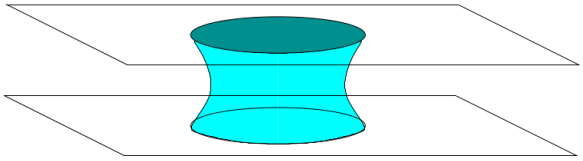

Figure 1. Plates and catenoid bridge.

one of the plates is tilted a small amount the soap film will slide to the edges of the plates that have the narrowest distance between them.

One practical application of this property of thin films in engineering is found in liquid propellant tanks. Unlike soap bubbles, a liquid drop can bridge non-parallel plates that form a small angle. Increasing this angle is equivalent to increasing the tilt of the plates. Eventually, as in the case of the soap film described above, the liquid drop slides to the edges of the plates that have the least distance between them. A fuel supplier in the shape of a wedge can be used to access small quantities of fuel as needed (Figure 2). By increasing the angle of the wedge, the fuel slides to the outlet of the supplier. Then the angle of the wedge can decrease again, so that another small portion of fuel is launched into the supplier, and then the supplier waits for the next access. This process is analogous to a pair of bellows that expels fuel instead of air.

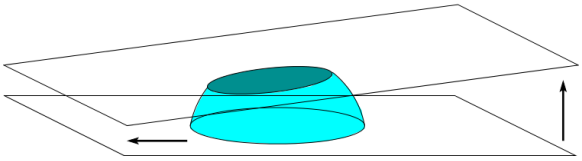

Figure 2. A liquid propellant tank.

Another factor that influences the way a liquid drop moves when the angle is varied is the so-called *wetting property* of each plate (Good, 1992). This can be described as a balance between how much the drop keeps its own cohesion and how much it adheres to a contact surface. Wetting and contact forces together produce an important effect called *capillarity*, which we mention in the next section.

The focus of the work discussed in this paper is using computational techniques to model the phenomenon of a bubble or liquid drop as it slides to the narrowest side between two tilted plates. In order to build our model we made use of a publicly available computer program called *Surface Evolver*. This program was created by Kenneth Brakke, professor at Susquehanna University, Department of Mathematical Sciences (USA). *Surface Evolver* allows the simulation of physical experiments in a virtual environment, and its source code is fully open (Brakke, 1994, susqu.edu/brake). In the next section we explain the strategies that were used to write the code of our simulator.[1]

METHODS

Surface Evolver reads data files that specify parameters, quantities, constraints, geometrical elements and scripts. In order to

DOI: http://dx.doi.org/10.7710/2168-0620.1064

write the data file that will simulate the phenomenon of interest for this work, the problem must be first described from a mathematical point of view.

This phenomenon can be described mathematically using a few geometrical properties. In doing so, some simplifying assumptions are made such as ignoring the thickness of the soap bubble, gravity applied to the liquid drop, etc. Even with these approximations, the essential ideal properties of the phenomenon can be understood.

The first requisite geometrical property is called *mean curvature*. Consider a point p in a smooth surface S. For each plane P that contains the normal line n to S through p, we have a planar curve $S \cap P$.

Of course, the set of all such planes can be parameterized by q in the interval [0,p] with P(0) = P(p). The curvature of $P(q) \cap S$ at p is a continuous function k(q) that attains its minimum k_1 and maximum k_2 within the compact interval [0,p] (Figure 3). The mean curvature of S at p is defined as $H(p) = (k_1+k_2)/2$.

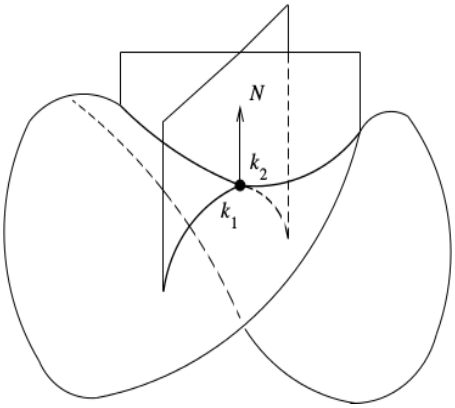

Figure 3. Maximum and minimum of k(q). N denotes the unitary normal vector that corresponds to the normal line n to S through p.

The second requisite geometrical property is the contact angle between the drop and the plates. Liquids are endowed with capillarity, a concept that is beyond the scope of this paper. However, mathematically speaking, this means that a drop that is rotationally invariant around an axis of symmetry makes a constant angle with its surface of contact. Rotational invariance does not apply to our configuration, but we will take *constant contact angle* as a simplification of our model. In practice, the contact angle is *not* constant. The (external) contact angle increases when we approach the apex of the wedge. This is the point that advances to the apex, and for this reason it is called *advancing contact angle*. It decreases when we approach the opposite point of contact, where we have the *receding contact angle* (Luo et al., 2014). Of course, this is what happens when the wetting property is *uniform* on the whole surface of contact. We could get a constant contact angle if the wetting property had a suitable variation over that surface.

Figure 4 shows the geometry of interest in this paper. We consider that the contact angle γ_1 between the drop S and the upper plate Π_1 has a *constant value* throughout the intersection $S \cap \Pi_1$, and the same holds to the contact angle γ_2 between S and the lower plate Π_2. We call α the angle between the plates.

Of course, by neglecting gravity we should a priori have $\gamma_1 = \gamma_2$. But this is still not the case if we consider that the plates have different wetting properties. Hence, in our simulations their constant values are not necessarily equal.

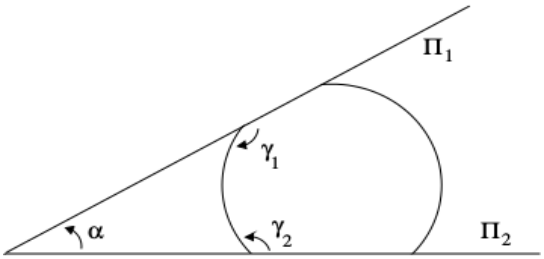

Figure 4. Constant angles of contact.

It is important to notice that Figure 4 shows a profile not in accordance with Luo et al. (2014), who conclude that both γ_1 and γ_2 should be acute. However, soon we will present Theorem 1 of McCuan (1997), which states that under certain hypotheses we cannot have $\gamma_1 + \gamma_2 \leq \pi + \alpha$, and

DOI: http://dx.doi.org/10.7710/2168-0620.1064

consequently $\gamma_1 + \gamma_2$ cannot be less than π. This contradiction occurs because the theorem refers to a mathematically ideal model that includes some simplifications.

McCuan (1997) establishes S, Π_1, Π_2, γ_1, γ_2 and α as above. Moreover, he supposes that γ_1, γ_2 have constant values and that S is *embedded* and has *constant mean curvature*. In our context *embedded* simply means "without self-intersections."

The hypothesis of embedding has to do with the fact that, in nature, we do not typically find drops with knots. There *are* soap films with self-intersections. If a closed wire is dipped into a soap solution the resulting soap film is not generally embedded. However, this is a special case and not one that is relevant for this work.[2]

The hypothesis of constant mean curvature (HCMC) is grounded in a physical experiment that was first performed by the French mathematician Jean Baptiste Meusnier in 1776. His experiment consisted of observing the behavior of an elastic membrane in the middle of a glass tube. He could inject and remove gas either above or below the membrane, so that each level was under different *constant* pressures P_1 and P_2. The membrane spanned a non-planar curve, as depicted in Figure 5.

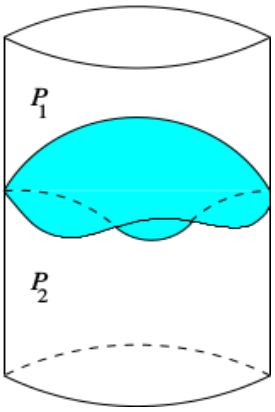

Figure 5. Elastic membrane in a glass tube.

Meusnier observed that $P_2 - P_1 = \lambda H$, where λ is a constant that depends only on the material and the thickness of the membrane. Namely, the surface that separates two ambients at pressures P_1 and P_2 has *constant* H. In the case of a drop the liquid is denser than the surrounding air. The effect is the same, and so the surface S of the drop has constant H. For a soap film, however, $P_2 = P_1$ and what we have is a so-called *minimal surface* S. Notice that in this case S is *concave* (see Figure 1) and that $k_1 = - k_2$. This characterizes saddle points (see Figure 3).

Because of these particularities, and using the term *ring type surface* to denote a topological annulus, McCuan (1997) assumes that S is of ring type and also verifies the following hypotheses: it is an embedded surface of constant H which spans a wedge of opening angle α and meets the planes Π_1 and Π_2 of the wedge at constant contact angles γ_1 and γ_2, respectively. With this setting he proves

Theorem 1. *No embedded ring type spanner* S *of constant H and constant contact angles can exist if* $\gamma_1 + \gamma_2 \leqslant \pi + \alpha$.

Theorem 2. *A spherical spanner exists if and only if* $\gamma_1 + \gamma_2 > \pi + \alpha$. *Letting* $A > 0$ *denote either enclosed volume or mean curvature, the family of all spanning spheres may be indexed uniquely by the set of 4-tuples* $(\gamma_1, \gamma_2, \alpha, A)$ *for which this existence criterion is satisfied*.

Of course, spherical rings S clearly verify the inequality of Theorem 2. The strength of this theorem resides in its second statement, for it characterizes any spherical ring by means of a 4-tuple. Now, if S has constant H and is a compact embedded ring type spanner in a wedge, and also meets the planes of the wedge in constant angles along its boundary, then S must be a spherical ring according to (Park, 2005).

In Theorem 2, notice that A can be either H or Vol(S). In fact, either of these two quantities determines the other because $\mathrm{Vol}(S) = - \pi/(3H^3)\cdot[\cos\gamma_1\ (2 + \sin^2\gamma_1) + \cos\gamma_2\ (2 + \sin^2\gamma_2)\ ]$. This equation does not

DOI: http://dx.doi.org/10.7710/2168-0620.1064

depend on α, which is however necessary to determine the spherical ring.

As mentioned previously, we assume that gravity is negligible for both soap films and drops. Of these, liquid drops would be the most massive. A drop has a volume of about 50ml. If we assume it is made of mercury, one of the densest liquids (13.6kg/m^3), then it weighs just 0.68 mg. In order to see that it is negligible, just change lines 1 and 88 of our datafile as we will explain below.

Our datafile **sdrop.fe** begins as follows:

```
GRAVITY_CONSTANT 0.0

PARAMETER va   = pi/6
PARAMETER gam1 = pi/2+1
PARAMETER mcv  = 1
PARAMETER fa   = va
PARAMETER gam2 = pi+fa+0.5-gam1

#define av -pi/(3*mcv^3)*(cos(gam1)'
*(2+(sin(gam1))^2)+cos(gam2)*(2+'
(sin(gam2))^2))
```

These are initial values like `va` (variable alpha), `fa` (fixed alpha), `mcv` (mean curvature) and `av` (annulus volume). In *Surface Evolver* we usually call "parameter" a value that does not depend on a formula. The value of a defined macro is always computed through a formula. Interaction with the *Surface Evolver* is via command line at a prompt. Hence, at the *Surface Evolver* prompt you can invoke and change `va`, `fa`, etc. by typing `print mcv`, `gam1 := pi/1.8`, etc. The macro `av` is *not* recognized at the prompt but only internally by the program. The symbol ' means "line break". In *Surface Evolver* you turn gravity on by replacing the above `0.0` with `1.0`.

Next in our datafile we have:

```
quantity fvol fixed = av'
method facet_vector_integral
vector_integrand:
q1: x
q2: 0
q3: 0
```

This means that Evolver will try to construct a triangulated surface with volume as close as possible to `av`. Namely, we will work with a triangulated surface and the more triangles we have, the more precise is the computed volume. Although fixed, whenever we change `mcv`, `gam1`, etc., `av` is re-calculated and gives a new fixed value for `fvol`. This quantity will be computed with `method facet_vector_integral` as follows:

$$\int_S (q_1, q_2, q_3) \cdot N dS \overset{\text{Gauß}}{=} \int_V div(x, 0, 0) dV$$

$$= \int_V \Big(\frac{\partial x}{\partial x} + 0 + 0\Big) dV = \int_V 1\, dV = \mathtt{av}. \qquad (1)$$

In applying Gauss' Theorem in (1), the ring type spanner S can only comprise a closed volume if we add the circles C_1 and C_2 that correspond to $S \cap \Pi_1$ and $S \cap \Pi_2$, respectively. If added to the surface integral in (1), their integrand would be (x, 0, 0) · (0,-sin α, cos α) = 0 over C_1 and (x, 0, 0) · (0, 0,-1) = 0 over C_2.

Our choice of the integral field q_1, q_2, q_3 allows *Surface Evolver* to compute the volume by numerical integration over S.

Next in our datafile we have:

```
constraint 1 /* over Pi 2 */
formula: z = 0
energy:
e1: cos(gam2)*y
e2: 0
e3: 0
```

The reason for these commands is the same as explained by Brakke (1994). But for the convenience of the reader we will detail it here. Notice that Π_2 is equated as `z=0`, and the surface tensions T_1, T_2 over C_1 and C_2, respectively contribute to the overall energy that *Surface Evolver* seeks to minimize. This energy acts on the closed surface $S \cup C_1 \cup C_2$, but in Section 3.3 of Brakke (1994) the author explains the convenience of omitting

DOI: http://dx.doi.org/10.7710/2168-0620.1064

additional parts like C_1 and C_2, and working with line integrals along their boundaries in order to get the same numerical values. Because of that we will compute the surface integrals over C_1 and C_2 by means of Stoke's Theorem. The surface tension that acts on C_2 corresponds to the force $(0,0,T_2)$, where $T_2 = -\cos\gamma_2$. Therefore,

$$\int_{C_2}(0,0,T_2)\cdot d\vec{S} = \int_{\partial C_2}(-T_2 y,0,0)\cdot d\vec{t}. \quad (2)$$

Similarly, Π_1 is equated as `z=tan(va)*y` and over C_1 the surface tension corresponds to $(0,-T_1 \sin\alpha, T_1\cos\alpha) = T_1$ N, where N is the unitary normal and $T_1 = \cos\gamma_1$. Now we choose (e_1, e_2, e_3) in such a way that the dot product of its rotational field with N will result in T_1:

```
constraint 2 /* over Pi 1 */
formula: z = tan(va)*y
energy:
e1: cos(gam1)/sin(fa)*z
e2: 0
e3: 0
```

The final three constraints are purely geometrical:

```
constraint 3
formula: x = 0

constraint 4
formula: x = 3
constraint 5
formula: y^2+z^2 = 9
```

They mean that we will display both Π_1 and Π_2 as squares of edge length 3, and Π_1 can only vary inside the cylinder $y^2 + z^2 = 9$.

Now we define a prototype of S: a polyhedral ring surface with 4 facets. It looks like a bottomless box without a lid. *Surface Evolver* displays it as in Figure 6.

In order to define this prototype we begin by declaring its vertices.

```
vertices
1 1.0 1.0 0.0 constraint 1
2 2.0 1.0 0.0 constraint 1
3 2.0 2.0 0.0 constraint 1
```

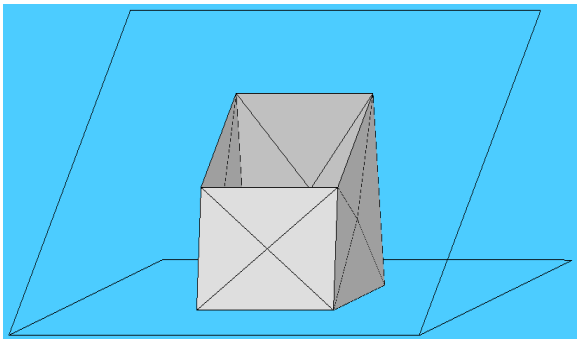

Figure 6. Prototype of our model.

```
4 1.0 2.0 0.0 constraint 1
5 1.0 1.0 1.0 constraint 2
6 2.0 1.0 1.0 constraint 2
7 2.0 2.0 1.0 constraint 2
8 1.0 2.0 1.0 constraint 2
```

The vertices that represent Π_2 by a 3×3 square must come in the sequel:

```
 9 0.0 0.0 0.0
           constraints 1,2,3 fixed
10 3.0 0.0 0.0
           constraints 1,2,4 fixed
11 3.0 3.0 0.0
           constraints 1,4,5 fixed
12 0.0 3.0 0.0
           constraints 1,3,5 fixed
```

Notice that vertices 9 and 10 are shared with the 3×3 square that represents Π_1. Therefore, we only need to add another two vertices.

```
13 3.0 3*cos(va) 3*sin(va)
           constraints 2,4,5 fixed
14 0.0 3*cos(va) 3*sin(va)
           constraints 2,3,5 fixed
```

After having defined the vertices we need to list the edges, faces and bodies (*body* is the term that *Evolver* uses to link facets as parts of the same object). For the sake of conciseness they will be omitted here.

At line 88 of our datafile **sdrop.fe** the reader can add `density 0.0136` to the body. This corresponds to a mercury drop as commented beforehand. Now, by running the simulation with `GRAVITY_CONSTANT 1.0` the reader will not see any significant

DOI: http://dx.doi.org/10.7710/2168-0620.1064

changes in volume, area or shape of the surface. That is why we can neglect gravity.

In the next section we explain some of our scripts, which will make the initial surface evolve to a spherical annulus S, vary the angle between Π_1 and Π_2, and show how this affects S in a dynamic way.

RESULTS

In the Methods section we discussed the beginning of our datafile, in which important parameters are defined, especially the mean curvature `mcv` and the annulus volume `av`. Notice that `mcv` is only used to define `av` and does *not* appear elsewhere in the code. Thus, we could have fixed a numerical value for `av` and the simulation would have given the same output *independent* of the HCMC.

Moreover, our simulation gives evidence that S must be spherical, a fact that was formally proved by Park (2005) but *still* under the HCMC. According to the results of our program, the HCMC may be unnecessary. However, many theoretical results rely on it, perhaps as a means of making progress in otherwise extremely difficult proofs. For instance, we cite:

1. Concus et al. (2001) deal with instability of tubular liquid bridges between parallel plates.

2. Finn (2002) lists and proves eight geometrical and physical properties regarding capillarity.

3. Luo and Heng (2014) describe the invention of a technique to separate oil from water by pressing plates on the mixture. The perfect separation relies on the difference of pressure inside the liquid drop. In our mathematical model we could add different *constant* mean curvatures to simulate the effect of these different pressures.

Such simplifications have already shown some contradiction with what happens in practice, as mentioned in the Methods section. However, *Surface Evolver* allows additional complexity beyond the simple example shown in this work. For professional purposes, we believe that *Evolver* achieves virtual simulations that can come much closer to what is observed in real experiments.

We mentioned the wetting property in the Introduction section and our program apparently neglects that important parameter. However, in the Methods section we explained that, although in practice the angles γ_1 and γ_2 are not really constant, the fact that we can take γ_1 different from γ_2 is a way of considering an *effect* of the wetting property. Hence, despite our simplifications we take that property into account by considering one of its effects.

Therefore, our code is very likely to improve both the theoretical and practical techniques that rely on the HCMC. Namely, from the numerical point of view, spherical surfaces of constant mean curvature automatically arise.[3]

DISCUSSION

We have presented a simple physical experiment simulated with *Surface Evolver*. Such an experiment can be easily reproduced in a laboratory but perhaps only for the special case of soap bubbles. Drops are too small to work with, and in fact our practical example in engineering, given in the Introduction section, includes a narrow slot at the apex of the wedge. We will implement this slot in future work.

Moreover, notice that we cannot force prescribed angles γ_1 and γ_2 for a soap bubble without the addition of extra constraints as has been demonstrated using soap films and loops of thread.[4] Each thread will assume the fixed shape of a circumference and so we cannot use our simulator to show what happens when α varies above the threshold. Namely, the exact case in which both circles C_1 and C_2 turn out to be tangent to each other.

DOI: http://dx.doi.org/10.7710/2168-0620.1064

We hope to have motivated students and professionals to use the Surface Evolver as a virtual environment for their physical experiments.

REFERENCES

Brakke, K. A. (1994). Surface Evolver Manual. Minneapolis, United States: Geometry Center, University of Minnesota. URL: www.susqu.edu/brakke/evolver/downloads/manual270.pdf

Concus, P., Finn, R., and McCuan, J. (1999). Liquid bridges, edge blobs, and Scherk-type capillary surfaces. *Indiana University Mathematics Journal*, 50(1), 411–442. DOI: http://dx.doi.org/10.1512/iumj.2001.50.1849

Finn, R. (2002). Eight remarkable properties of capillary surfaces. *The Mathematical Intelligencer,* 24(3), 21–33. DOI: http://dx.doi.org/10.1007/BF03024728

Good, R. J. (1992). Contact angle, wetting, and adhesion: a critical review. *Journal of Adhesion Science and Technology*, 6(12), 1269–1302. DOI: http://dx.doi.org/10.1163/156856192X00629

Isenberg, C. (1978). The science of soap films and soap bubbles. Courier Corporation.

Luo, C., Heng, X., and Xiang, M. (2014). Behavior of a liquid drop between two nonparallel plates. *Langmuir*, 30(28), 8373–8380. DOI: http://dx.doi.org/10.1021/la500512e

Luo, C. and Heng, X. (2014). Separation of oil from a water/oil mixed drop using two nonparallel plates. *Langmuir,* 30(33), 10002–10010. DOI: http://dx.doi.org/10.1021/la501804h

McCuan, J. (1997). Symmetry via spherical reflection and spanning drops in a wedge. *Pacific Journal of Mathematics,* 180(2), 291–323. DOI: http://dx.doi.org/10.2140/pjm.1997.180.291

Park, S. (2005). Every ring type spanner in a wedge is spherical. *Mathematische Annalen*, 332(3), 475–482. DOI: http://dx.doi.org/10.1007/s00208-005-0476-2

[1] Our code is named **sdrop.fe** and can be downloaded from our homepage https://sites.google.com/site/chrondon1992 but it needs installation of Evolver 2.70 to run, preferably in the operating system Linux Ubuntu 14.04 or higher. The user can install the older version 2.30 through the Ubuntu software center. Alternatively, just enter the command line **sudo apt-get install evolver** at the terminal prompt.

[2] See susqu.edu/brakke/knots for some illustrations.

[3] Here we show how to perform the simulation. Our main scripts are: **gogo**, **olid** and **omre**. Basically, each of them consists of a list of single-letter commands, of which the meanings are explained by Brakke (1994). Therefore, we will omit details here and focus on the functionality of our scripts.

Now you should install Evolver and download our file **sdrop.fe**, as explained at the Introduction. Open a terminal, go to the directory where **sdrop.fe** is and then type **evolver sdrop** at the prompt. You will get an interactive picture as illustrated in Figure 6. Now run the first script at the Evolver prompt, which is **gogo**. This script refines and smoothens our prototype until we see a virtual drop inside the wedge, as depicted in Figure 7.

The opening of the virtual wedge is $\alpha = \pi/6$. In the datafile **sdrop.fe** there are two variables that refer to α, namely `va` and `fa`. Their names are a mnemonic to variable and fixed alpha, respectively. We made this distinction in order for our next scripts to open the wedge by increasing the value of `va`. However, we keep `fa` fixed because the values of γ_1 and γ_2 are fixed and satisfy the equality $\gamma_1 + \gamma_2 = 0.5 + \pi + \alpha$, for the initial value `fa` of α. In the datafile they are

DOI: http://dx.doi.org/10.7710/2168-0620.1064

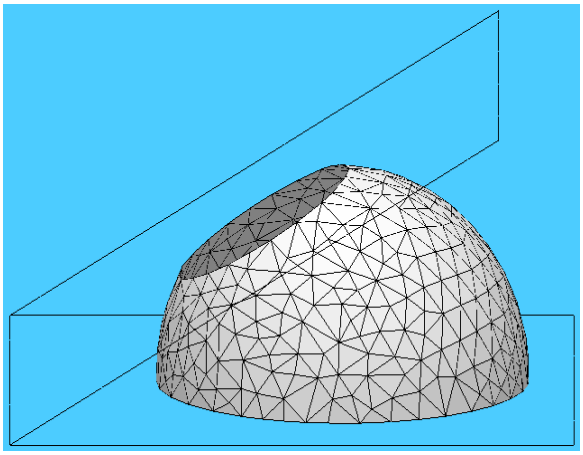

Figure 7. Virtual drop inside the wedge.

mcv = 1, **gam1 = pi/2 + 1** and **gam2 = pi + fa + 0.5 – gam1**, respectively. With this setting we begin our simulation according to Theorem 2. The inequality $\gamma_1 + \gamma_2 > \pi + \alpha$ is equivalent to `va < fa + 0.5`, which is true at the beginning since `va = fa =` $\pi/6$.

Now run the script **olid**, which will "open the lid" P_1 at `va =` $\pi/5$ (Figure 8).

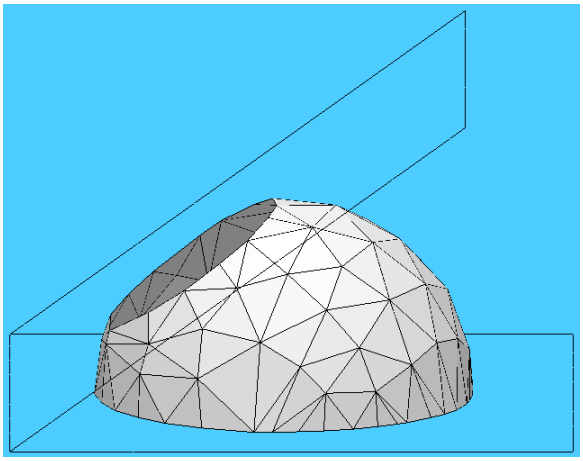

Figure 8. Wedge opened to $\pi/5$.

You can open it a bit more with **omre**, for which `va` $= \pi/4$ (Figure 9). The threshold `va = fa =` $\pi/6$ (Figure 10) is arrived at by running **thrs**.

The reader must have noticed that Fig. 7 is more refined than the subsequent ones. We did this on purpose because the scripts **olid**, **omre** and **thrs** aim at arriving at the threshold. Therefore, refining the picture for each of these steps would increase the computational cost. Moreover, it is possible

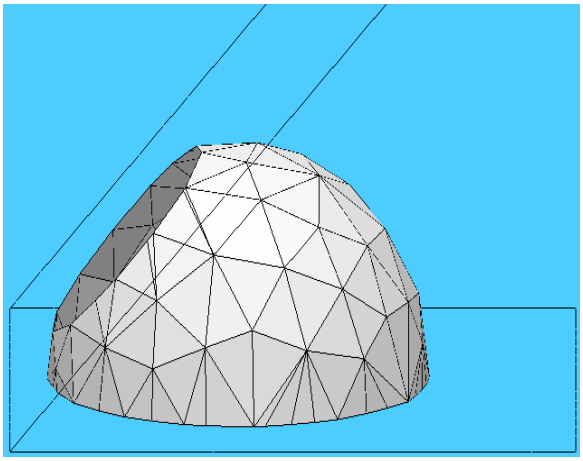

Figure 9. Wedge opened to $\pi/4$.

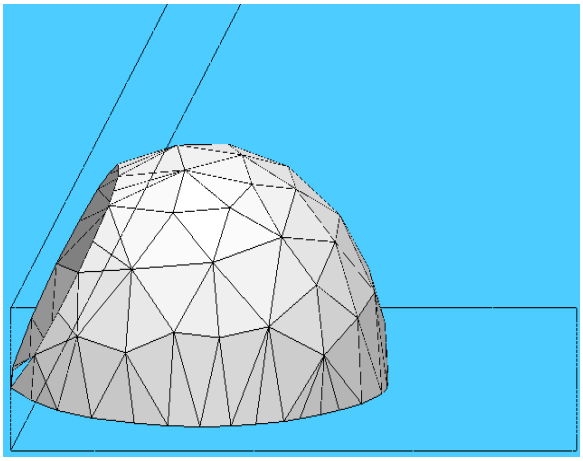

Figure 10. Threshold at `va = fa =` $\pi/6$.

to enhance and create an animation with them by means of a viewing program, for instance *Geomview*. The reader can access the animation file **sdrop.mp4** at our homepage.

Finally, according to Theorems 1 and 2 we can determine when the ring type spanner drop will cease to exist. Figure 11 shows the case $\alpha =$ `va<fa+`$0.5 = \gamma_1 + \gamma_2 - \pi$.

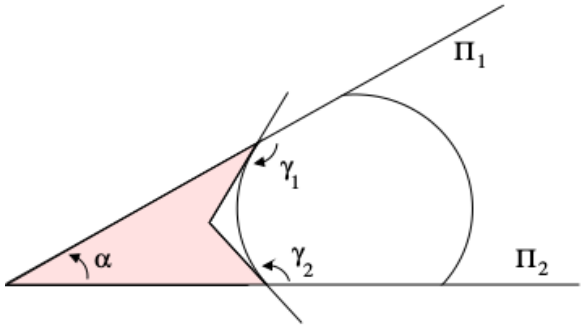

Figure 11. Concave quadrilateral.

DOI: http://dx.doi.org/10.7710/2168-0620.1064

There the shaded quadrilateral is concave and the sum of the three internal angles $\pi - \gamma_1$, $\pi - \gamma_2$ and α is less than π.

As α approaches `fa` + 0.5 the concave quadrilateral converges to an infinitesimal triangle for which we finally have $\alpha = g_1 + g_2 - \pi$.

By increasing α further on the ring pops and assumes the shape of a half- moon. This can be seen by running the script **brst** of our simulator (Figure 12).

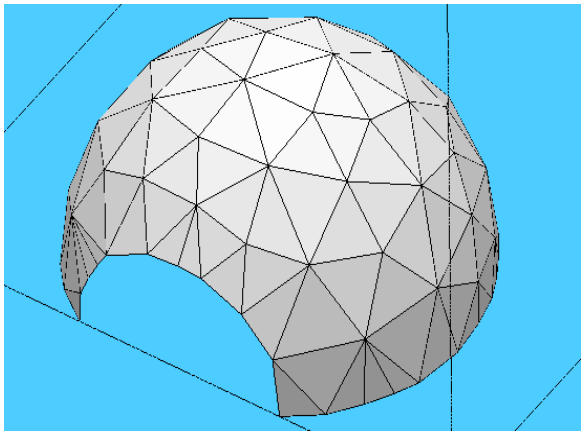

Figure 12. Ring is replaced by half-moon.

Finally, the scripts **aflt** and **flat** are two steps that show what happens to the half-moon when we open α until the extreme value π. This can be seen in the video **sdrop.mp4** linked from our homepage: https://sites.google.com/site/chrondon1992. We end up with a spherical cap that makes an internal angle γ_2 with the horizontal plane. The upper arc of the half-moon collapses to a single point on the line that separates Π_1 and Π_2.

[4] An example can be seen in the video **Soap Film Loops.mp4** on our homepage https://sites.google.com/site/chrondon1992, taken from the publicly available *Harvard Natural Sciences Lecture Demonstrations*.

DOI: http://dx.doi.org/10.7710/2168-0620.1064